Trap profiling at nanocavity bands in silicon wafers by means of capacitance–voltage measurements

2002 J. Phys.: Condens. Matter 14 13087

(http://iopscience.iop.org/0953-8984/14/48/354)

J. Phys.: Condens. Matter **14** (2002) 13087–13094 PII: S0953-8984(02)54060-1

Trap profiling at nanocavity bands in silicon wafers by means of capacitance–voltage measurements

Nicolas Auriac and Santo Martinuzzi

UMR TECSEN 61-22, University of Aix-Marseille III, 13397 Marseille Cedex 20, France

Received 27 September 2002
Published 22 November 2002
Online at stacks.iop.org/JPhysCM/14/13087

Abstract

Nanocavities are formed by He^+- and H^+-ion implantation in silicon single crystals, at the projected range R_p, after post-implantation annealing. The present paper deals with the characterization of deep trap levels associated with such defects.

P-type silicon single crystals were implanted using He^+- and H^+-ion beams, at an energy of 250 keV and to a dose of 3×10^{16} cm^{-2}. Capacitance–voltage (C–V) profiling and deep-level transient spectroscopy (DLTS) techniques were used to determine the density profile and the energy levels of deep traps in the gap.

In implanted and post-annealed samples a quasi-triangular profile of the space charge is revealed around R_p by C–V profiling, and the space charge density reaches 10^{16} cm^{-3}. DLTS suggests that trap levels are located at 0.4 eV above the valence band, with a maximum density around 10^{15} cm^{-3} at R_p.

The sign and distribution of the space charge for depletion in He^+-implanted samples are indicative of the presence of acceptor-like deep traps induced by cavities, irrespective of metallic contaminations, which can be due mainly to dangling bonds.

1. Introduction

It is well known that helium-ion implantation in silicon at doses exceeding 2×10^{16} cm^{-2} produces bubbles beneath the implanted surface around the ion projected range R_p which depends mainly on the ion energy. Subsequent annealing at a temperature $T > 700$ °C causes the exodiffusion of He, leaving a band of nanocavities around R_p [1]. We obtained similar results by means of hydrogen-ion implantation provided that here again the ion dose exceeds 2×10^{16} cm^{-2}.

The internal surfaces of such nanocavities have been recognized as creating dangling bonds and trapping impurity atoms, like metallic fast diffusers. As a consequence, a non-homogeneous distribution of deep trap levels is formed beneath the implanted surface, which can be ascribed to implantation defects and to cavity surfaces and associated defects such as dislocation loops. However, as many implantation defects disappear during the subsequent

0953-8984/02/4813087+08$30.00

annealing performed to form the cavities, traps are essentially concentrated within the cavity band and their distribution is assumed to be triangular. Nevertheless, it is emphasized that the presence of the voids does not alter the material dielectric constant. This is due to the small size of the cavities, which will be considered as large extended defects.

Dangling orbitals in silicon can be either positively or negatively charged, like in vacancy defects, and cavities may be electrically active and develop a buried space region around R_p. This buried layer creates a potential barrier of several tenths of an electron volt, like around grain boundaries [2], and induces a band bending which is repulsive for majority carriers. The nanocavity region could behave like an insulator with a dielectric constant $\varepsilon_r = 11.9$.

In the present paper we report an investigation of electrical properties of the deep traps located within the bulk at micrometre depths in the cavity region. The electrical diagnostic tools are capacitance versus voltage (C–V) plots and deep-level transient spectroscopy (DLTS) [3, 4].

2. Experimental details

P-type silicon wafers, boron doped in the range $N_a = (2\text{–}4) \times 10^{15}$ cm^{-3}, Czochralski grown, were implanted with He^+ or H^+ ions. The ion energy was 250 keV and the dose was 3×10^{16} cm^{-2}. The projected range R_p was expected to be 1.3 μm for He^+ and 2.7 μm for H^+. After implantation, the wafers were annealed at various temperatures between 700 and 950 °C and then quenched to room temperature.

Some wafers were contaminated with gold or chromium in-diffusion during the annealing. Such samples are used to investigate the effect of these impurities on the trap properties when they are segregated at the cavity walls. They are also used to localize the cavity band by secondary-ion mass spectroscopy (SIMS), because the accumulation of metallic atoms at the defects gives rise to concentrations above the limit of sensitivity of this analytical technique.

Metal–insulator–semiconductor (MIS) diodes were used for the C–V and DLTS measurements. The back ohmic contact was obtained by deposition of a 250 nm thick aluminium layer and subsequent annealing at 400 °C for 20 min. The rectifying front contact on the implanted surface resulted from the deposition of a 200 nm thick aluminium film (without subsequent annealing) on the native SiO_2 layer. MIS diodes were also made on cavity-free samples cut out from the same wafer.

C–V plots were obtained by means of the voltage modulation technique at a frequency of 1 MHz, when the applied voltage varied between 0 and −40 V. DLTS signals were measured at temperatures between 80 and 300 K.

3. Space charge model

Since implantation defects were not expected to be present in significant density after annealing above 700 °C, the measured electrical effects were mainly ascribed to the cavity walls, although dislocation loops surrounded the cavity band. Indeed it was reported that the number of dangling bonds associated with dislocation loops was 2–4 orders of magnitude smaller than that of those on the cavity walls [4].

Figure 1(a) shows a profile of the trap distribution $N_t(x)$ close to the space charge region, with deep traps localized at the cavity band. The induced band bending is shown in figure 1(b), where the structure is in equilibrium. When a MIS diode is formed on the implanted surface and is reverse biased, the space charge region W of the MIS diode is extended and can enter the cavity region ($W > X_1$). As a consequence the cavity charge may be modified by emission or capture of holes.

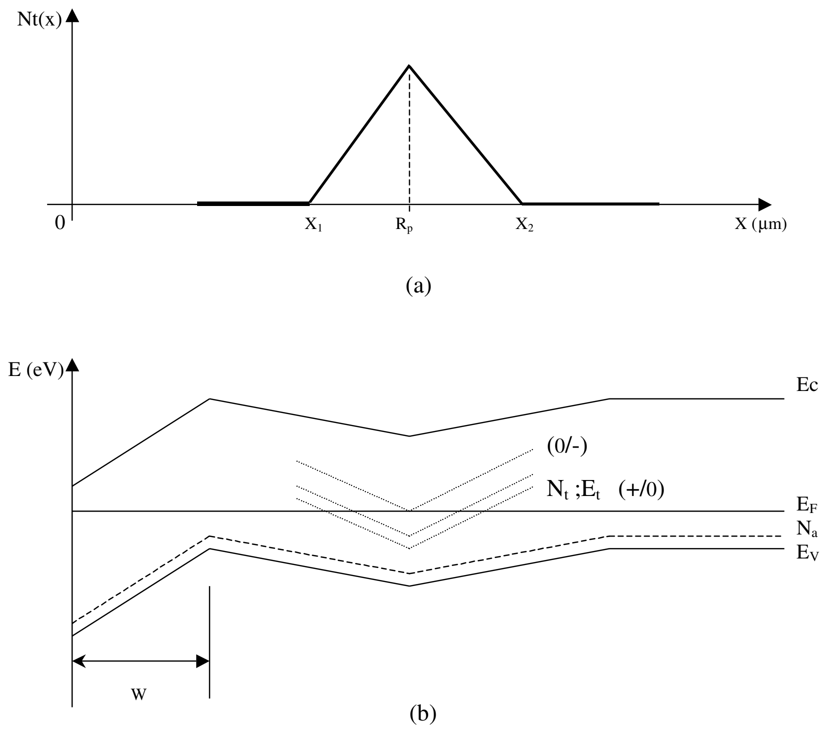

Figure 1. (a) The profile of the deep level associated with cavities around R_p, assuming a triangular distribution of voids. (b) The energy band diagram for when a MIS diode is formed on the implanted surface (no bias). Notice the band bending due to the cavities for $X_1 < X < X_2$ and to the edges of the cavity band.

If the deep traps are donor-like, C–V plots detect a space charge $\rho(x) = N_a - N_t(x)$ which follows the charge variation of the traps when the emission rate is high. Such a variation is due to the crossing of the trap energy E_t and Fermi levels E_F:

if $E_t < E_F$, the trap levels are neutral,

if $E_t > E_F$, the trap levels are positively charged.

When the emission rate is low, the traps remain neutral and C–V plots detect N_a over the entire space charge region.

For acceptor-like traps and if e_n is low, C–V plots detect $N_a + N_t(x)$ because the traps remain filled and negatively charged, like the acceptors, whatever the position of E_t compared with that of E_F. That is the case at high frequencies or at low temperature. For high emission rates the charge variation of the traps must be taken in account.

From C–V plots, the charge profile in the space charge region can be deduced.

4. Results

SIMS profiles detect gold or chromium atoms accumulated between 1 and 1.6 μm beneath the surface for He^+-implanted samples and between 2.25 and 3 μm for H^+-implanted ones, indicating that the cavity bands and associated defects are located around the expected values of R_p, as shown by figure 2.

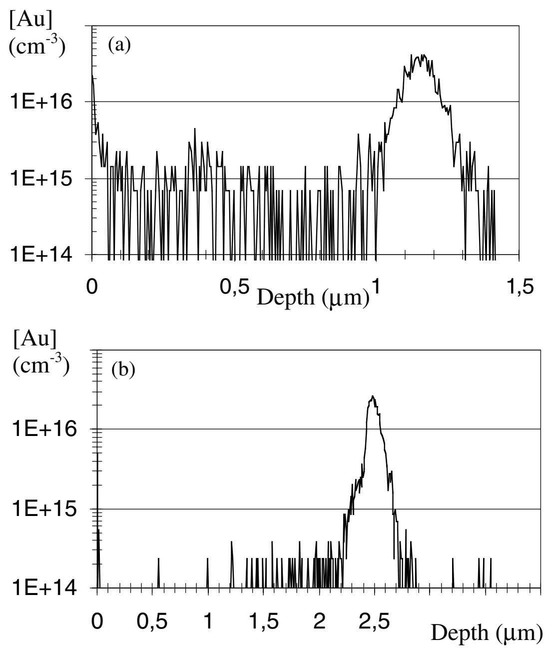

Figure 2. SIMS profiles of gold atoms beneath the implanted surface. (a) After He-ion implantation; (b) after H-ion implantation.

4.1. He⁺-implanted samples

Figure 3 shows a typical variation of the inverse square of the capacitance versus the reverse applied voltage for a cavity-containing sample and for a cavity-free one. The capacitance does not vary significantly in the cavity region, while when the depletion edge reaches depths beyond the cavity band, the slope of $1/C^2$ versus bias reverts to that related to the dopant density (which is that of the cavity-free sample). There is no variation of the $1/C^2$ curve from above to below the values for the cavity-free sample, indicating that there is no change in the charge sign with increasing reverse bias. Consequently the charge at cavities is negative, like that of acceptors.

Figure 4 shows the space charge profile $\rho(x)$ deduced from C–V curves plotted after annealing of the sample at various temperatures (T) between 700 and 950 °C.

After annealing at 700 °C, the profile is rather flat; the charge density, which is negative, is close to the doping level. Notice that at zero bias, the depletion region reaches 1.25 μm, probably because of residual implantation defects and to bubbles which give rise to the formation of a large compensated region beneath the implanted surface.

After annealing at $700 < T < 900$ °C, implantation defects tend to disappear, cavities are formed, and the negative space charge $\rho(x)$ increases between 1 and 1.6 μm, due to the contribution of cavities: $\rho(x) = N_a + N_t(x)$. Such a contribution may be ascribed to negative charge states of dangling bonds [4], which introduce acceptor-like traps, or to hole emission from the 0 state of the dangling bonds. As a consequence, the nanocavities in depletion are more negatively charged.

After annealing at $T \geqslant 900$ °C, sharp peaks appear in the profiles, which are probably artefacts due to a marked variation of the charge density over distances shorter than the Debye

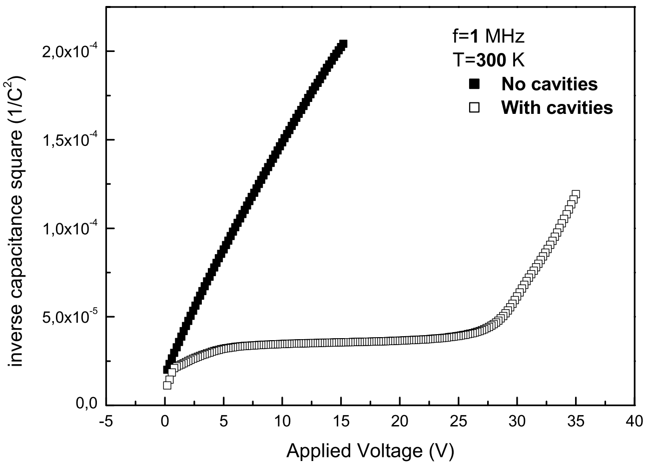

Figure 3. The inverse square of the capacitance versus the reverse applied voltage for a He-ion-implanted sample annealed at 950 °C for 2 h and quenched to room temperature.

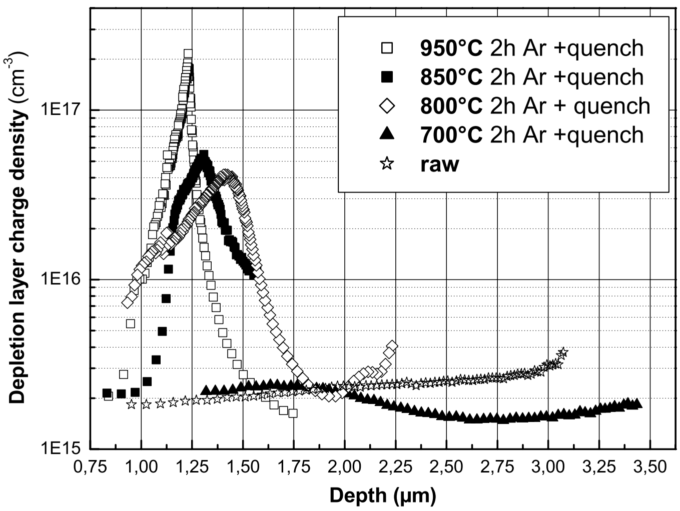

Figure 4. The depletion layer charge density beneath the implanted surface in He-implanted samples after annealing at various temperatures.

length: $L_D = (\frac{\varepsilon kT}{qN_a})$, with ε the permittivity and N_a the doping level. L_D is about 0.09 μm in the samples investigated.

The sharper variation of $\rho(x)$ at the limit of the cavity band in the samples annealed at $T \geqslant 900\,^{\circ}$C is certainly the consequence of the disappearance of points defects due to the implantation damage and to the cavity formation. Beyond the cavity band, $\rho(x)$ reverts to the doping level. As expected, in the cavity-free sample, $\rho(x) = N_a$.

No difference is observed in samples contaminated by Au or Cr atoms, although such impurities accumulate in the cavity band, suggesting that trapped atoms are included in neutral microprecipitates or complexes or simply trapped by dangling bonds.

When T is decreased from 300 to 175 K, the charge distribution of figure 4 shifts to the right, which is due to the extension of the depletion width and the decrease of the emission rate which becomes close to zero. At 85 K, $\rho(x)$ has reverted to the doping level.

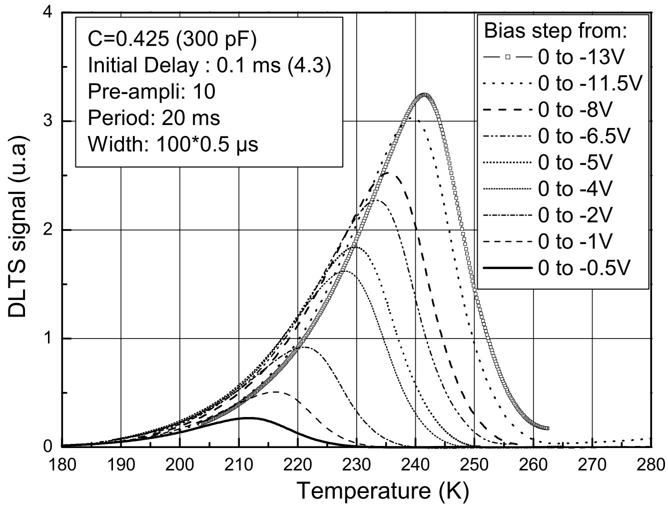

Figure 5. DLTS spectra of a He-ion-implanted sample for various bias voltages.

DLTS measurements on samples annealed at $T \geqslant 900\,^{\circ}$C detect a band of levels located at 0.45 eV above the valence band, with a very high mean capture cross-section for holes of a few 10^{-13} cm^2 and a density around 10^{15} cm^{-3}. The DLTS signal increases with the applied reverse bias, as shown in figure 5, indicating that the deep-level density increases with depth in the region between the implanted surface and the cavity band, i.e. between the edge of the depleted region at zero bias (about 0.9 μm) and the edge of the cavity band.

4.2. H^+-implanted samples

In H^+-implanted samples, $\rho(x)$ also increases in the cavity band around R_p and the cavities are formed at temperatures lower than that needed for helium-implanted samples, as $\rho(x)$ profiles are observed after annealing at $700\,^{\circ}$C, as shown in figure 6. However, some compensation occurs before the cavity band, and $\rho(x)$ decreases below the doping level, down to 6×10^{14} cm^{-3}. For such samples the curves $1/C^2$ versus applied reverse voltage cross that of a cavity-free sample at low voltage and confirm the existence of positive charges, opposite in sign to the acceptor atoms, as shown by figure 7.

This compensation may be due to the capture of holes by extended crystallographic defects, such as dislocation loops which are created during the cavity formation [6].

This compensation does not appear in the He-ion-implanted samples, probably because the edge of the MIS space charge region, W, is close to the cavity band and cavities are in depletion even at zero bias.

DLTS spectra reveal the presence of a broad band of deep levels located at 0.17 eV in the gap above the valence band with a capture cross-section around 10^{-17} cm^2.

The results concerning the H-ion-implanted samples are less clear than those for He-ion-implanted ones, because of the reactivity of hydrogen with the defects and because of the formation of blisters in the samples investigated [7].

5. Conclusions

Helium-ion implantation to doses higher than 2×10^{16} cm^{-2} gives rise to nanocavity band formation after subsequent annealing at temperature higher than $700\,^{\circ}$C. Capacitance

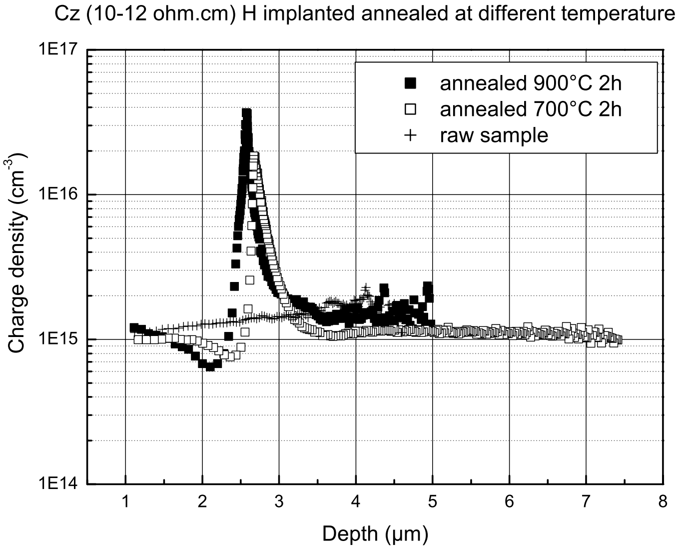

Figure 6. The inverse square of the capacitance versus the applied voltage for a H-ion-implanted sample annealed at 900 °C for 2 h and quenched to room temperature.

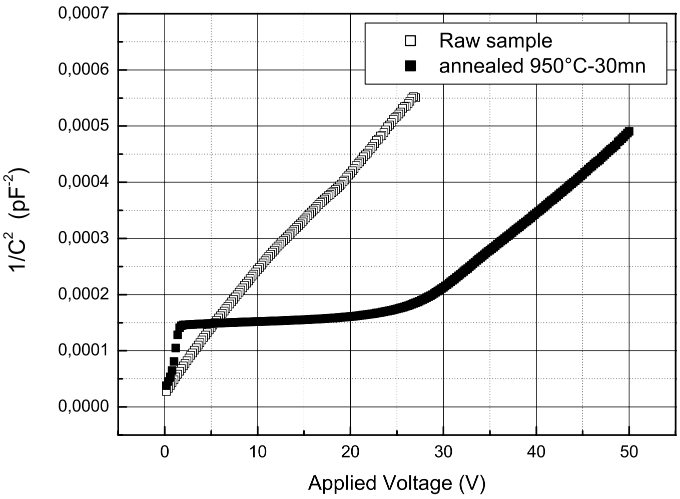

Figure 7. The depletion layer space charge density beneath the implanted surface in H-ion-implanted samples after annealing at various temperatures.

measurements reveal that a negative space charge profile appears in the cavity band which could be ascribed to the presence of acceptor-like deep trap levels mainly due to negative dangling bonds. Hole emission can also occur when the cavities are in depletion.

Hydrogen-ion implantations also create nanocavities upon annealing at temperatures between 600 and 700 °C, and a negative space charge profile is also observed in the cavity band.

The trapping of metallic atoms does not modify the charge profile in the cavity region, suggesting that such impurities are in an electrically neutral state.

Acknowledgments

This work was supported by CNRS-ECODEV and ADEME—France, and by the Conseil Général and Conseil Régional Région PACA—France.

References

[1] Griffioen C C, Evans J H, De Jong P C and Van Veen A 1987 *Nucl. Instrum. Methods Phys. Res.* B **27** 417–23
[2] Myers S M, Follstaedt D M, Stein H J and Wampler W R 1993 *Phys. Rev.* B **47** 13380–9
[3] Kimmerling L C 1974 *J. Appl. Phys.* **45** 1839–45
[4] Seager C H, Myers S M, Anderson R A, Warren W L and Follstaedt D M 1994 *Phys. Rev.* B **50** 2458–73
[5] Blood P and Orton J W 1992 *The Electrical Characterization of Semiconductors: Majority Carriers and Electron States* ed N H March (London: Academic) p 303
[6] Medernach J W, Hill T A, Myers S M and Hadley T J 1996 *J. Electrochem. Soc.* **143** 725–41
[7] Périchaud I, Yakimov E and Martinuzzi S 2001 *High Purity Silicon* vol 4, ed C Claeys, P Rai-Choudhury and M Watanabe (Pennington, NJ: Electrochemical Society) pp 341–6